

Manuscript Number:

Title: Highly Sensitive SERS Detection of Pb²⁺ Ions in Aqueous Media using Citrate Functionalised Gold Nanoparticles

Article Type: Research Paper

Keywords: Gold Nanosensor, Citrate, Lead, SERS

Corresponding Author: Dr. Debra Elayne Whitehead, Ph.D

Corresponding Author's Institution: Manchester Metropolitan University

First Author: Debra Elayne Whitehead, Ph.D

Order of Authors: Debra Elayne Whitehead, Ph.D; Mark S Frost, Chemistry; Michael J Dempsey, Microbiology

Abstract: Citrate functionalised gold nanoparticles (AuNPs) display strong surface enhanced Raman scattering, which can be used for surface enhanced Raman spectroscopy (SERS). The specific and strong interaction between the heavy metal ions and surface-bound citrate molecules lead to a sensing application for the detection of Pb²⁺ ions. Herein we report a citrate functionalised gold nanoparticle (AuNP) surface enhanced Raman spectroscopy (SERS) based sensor, employing the metal-affinity properties of the citrate molecule to detect Pb²⁺ ions. The Pb²⁺ ions interact with the citrate molecules via their carboxylate and hydroxyl groups altering the molecular spectra pertaining to the $\nu_{as}(\text{COO}^-)$, $\nu_{s}(\text{COO}^-)$ and $\nu(\text{C-OH})$ bands. The $\nu(\text{C-OH})$ band was used for the determination of the Pb²⁺ ion concentration. It decreased upon reducing the ion concentration and was found to be linear between 50 ng/L and 1000 ng/L with a 0.9982 correlation coefficient (R²) value. This method also showed good recovery and relative standard deviation (RSD) values.

Suggested Reviewers: Ewan Blanch Chemistry
Reader, Faculty of life sciences, Manchester University
e.blanch@manchester.ac.uk
Strong background in SERS

Colin Campbell Chemistry
Senior Lecturer, School of Chemistry, University of Edinburgh
colin.campbell@ed.ac.uk
Strong background in SERS nanosensors.

Mathias Brust Chemistry
Professor, Chemistry, University of Liverpool
M.Brust@liverpool.ac.uk
Pioneer of research using gold nanoparticles.

Duncan Graham Chemistry
Research Chair of Chemistry, Department of Pure and Applied Chemistry, University of Strathclyde

duncan.graham@strath.ac.uk

Surface Enhanced Raman Spectroscopy (SERS) : potential applications for disease detection and treatment

Karen Faulds Chemistry

Reader, Department of pure and applied chemistry, University of Strathclyde

karen.faulds@strath.ac.uk

Conducts research focused on using surface enhanced Raman scattering (SERS) to create new approaches to bioanalysis for use in the life and clinical sciences.



The Editor
Journal of Sensors and Actuators B

28th November 2014

Dear Sir/Madam

Please find attached a paper entitled: 'Highly Sensitive SERS Detection of Pb²⁺ Ions in Aqueous Media using Citrate Functionalised Gold Nanoparticles.'

by Mark S. Frost, Michael J. Dempsey, Debra E. Whitehead, for consideration as a '**regular article**' in your journal.

Mark Frost has carried out this work as part of his PhD research. The research has focussed on developing functional nanomaterials capable of detecting low level concentrations of a heavy metal identified as micro pollutant in Annex II of the Directive on Priority Substances (2008/105/EC). This investigation used gold and silver nanoparticles to determine interactions with heavy metals.

We believe that our work would be of great interest to your readers.

I certify that this manuscript, or any part of it, has not been published and will not be submitted elsewhere for publication while being considered by your journal. All authors have read and approved the manuscript.

Financial and competing interests disclosure: The work is partially funded by United Utilities PLC. No writing assistance was utilised in the production of this manuscript.

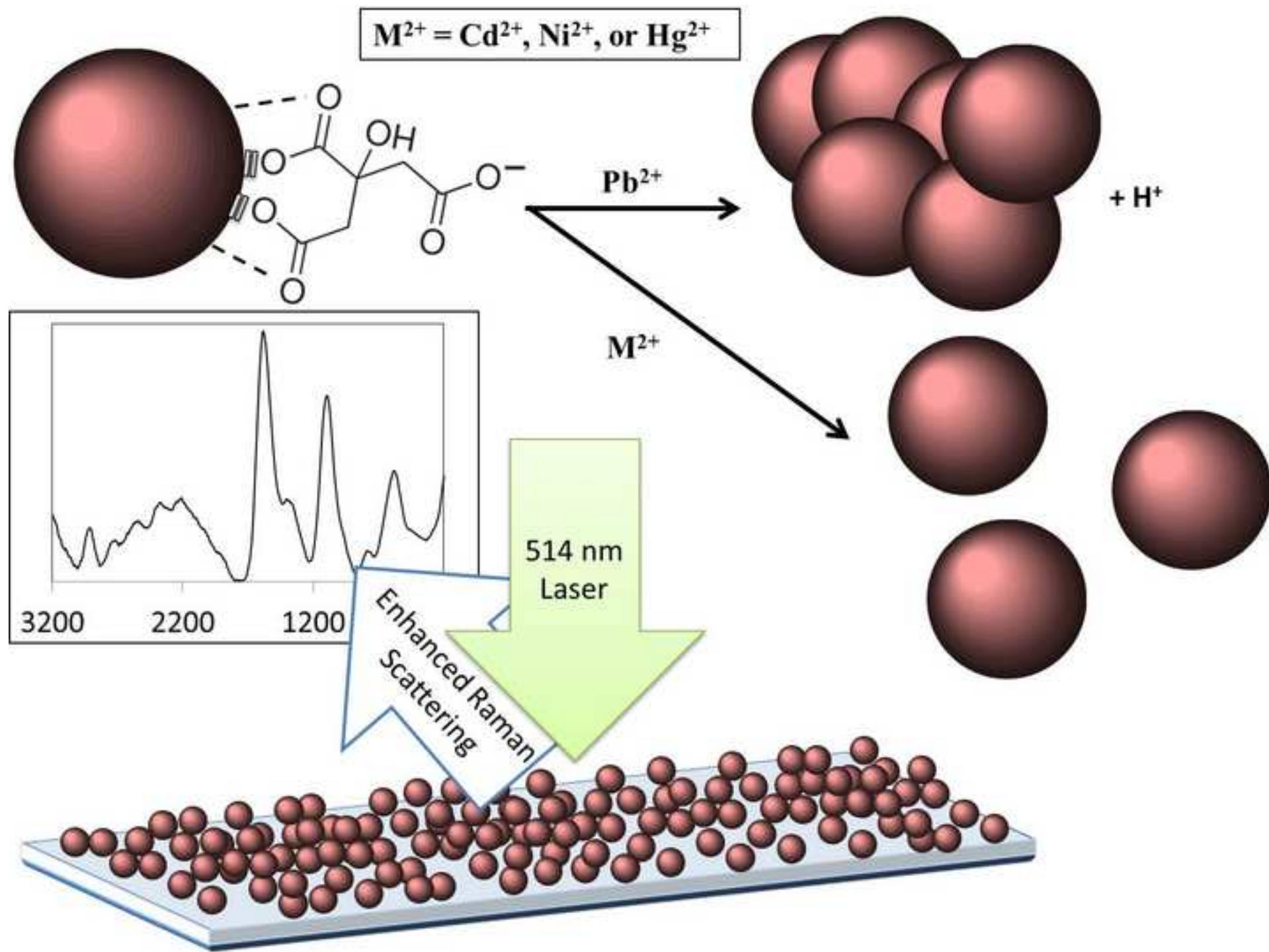
Conflict of interest: None.

I look forward to hearing from you soon.

Regards

Debra Whitehead

Dr. Debra Whitehead
School of Chemistry and the Environment
Manchester Metropolitan University
Manchester M1 5GD. United Kingdom.



Highlights

Herein we report a citrate functionalized gold nanoparticle (AuNP) surface enhanced Raman spectroscopy (SERS) based sensor employing the metal-affinity properties of the citrate molecule.

- Citrate functionalised gold nanoparticles (AuNPs) display strong surface enhanced Raman scattering which can be used for surface enhanced Raman spectroscopy (SERS).
- Their specific and strong interaction with heavy metal ions led to a sensing application for the detection of Pb^{2+} ions
- The Pb^{2+} ions interact with the citrate molecules via their carboxylate and hydroxyl groups altering the molecular spectra pertaining to the $\nu_{\text{as}}(\text{COO}^-)$, $\nu_{\text{s}}(\text{COO}^-)$ and $\nu(\text{C-OH})$ bands.
- The $\nu(\text{C-OH})$ band was used for the determination of the Pb^{2+} ion concentration: It decreased upon reducing the ion concentration and was found to be linear between 25 ng/L and 1000 ng/L with a 0.9676 correlation coefficient (R^2) value.
- This method showed good recovery and relative standard deviation (RSD) values.

TITLE: Highly Sensitive SERS Detection of Pb²⁺ Ions in Aqueous Media using Citrate Functionalised Gold Nanoparticles

Short running title: SERS detection of Pb²⁺ ions on gold nanoparticles.

Authors: Mark S. Frost, Michael. J. Dempsey, Debra E. Whitehead*

The School of Science and the Environment, Faculty of Science and Engineering, Manchester Metropolitan University, Manchester, M1 5GD, UK

Corresponding author:

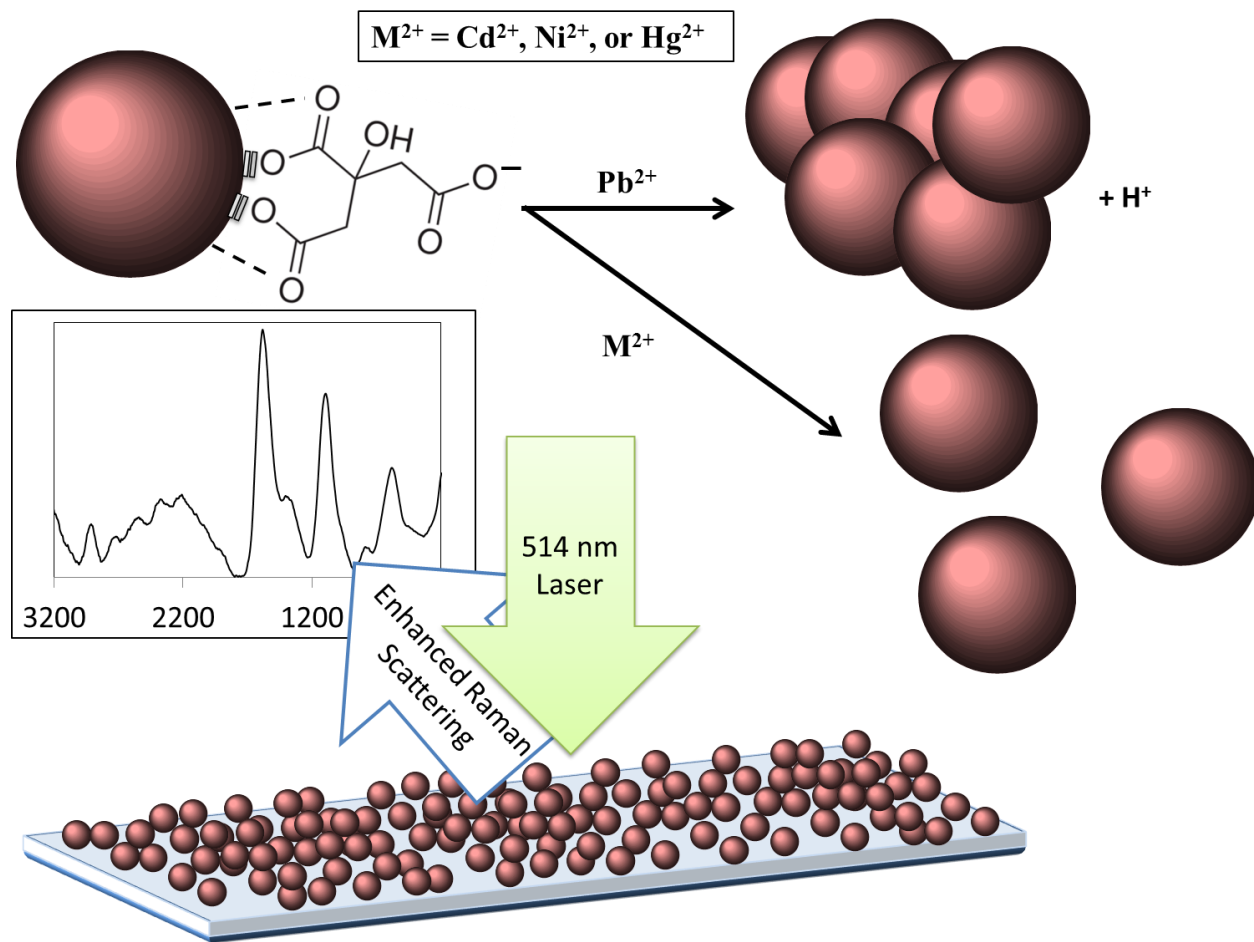
* Dr. Debra Whitehead, The School of Science and the Environment, Faculty of Science and Engineering, Manchester Metropolitan University, Manchester, M1 5GD, UK.

Tel +44 0161 247 3341, Email d.whitehead@mmu.ac.uk

ABSTRACT

Citrate functionalised gold nanoparticles (AuNPs) display strong surface enhanced Raman scattering, which can be used for surface enhanced Raman spectroscopy (SERS). The specific and strong interaction between the heavy metal ions and surface-bound citrate molecules lead to a sensing application for the detection of Pb²⁺ ions. Herein we report a citrate functionalised gold nanoparticle (AuNP) surface enhanced Raman spectroscopy (SERS) based sensor, employing the metal-affinity properties of the citrate molecule to detect Pb²⁺ ions. The Pb²⁺ ions interact with the citrate molecules via their carboxylate and hydroxyl groups altering the molecular spectra pertaining to the $\nu_{as}(\text{COO}^-)$, $\nu_s(\text{COO}^-)$ and $\nu(\text{C-OH})$ bands. The $\nu(\text{C-OH})$ band was used for the determination of the Pb²⁺ ion concentration. It decreased upon reducing the ion concentration and was found to be linear between 50 ng/L and 1000 ng/L with a 0.9982

correlation coefficient (R^2) value. This method also showed good recovery and relative standard deviation (RSD) values.



Keywords: Gold Nanosensor, Citrate, Lead, SERS

1. INTRODUCTION

Heavy metal pollutants detected in water can vary down to trace and ultra-trace concentration levels ($\mu\text{g/L}$ – ng/L). Despite these concentrations, the long-term exposure can have a serious impact on the environment and human health [1,2]. An infamous heavy metal pollutant is Pb which can be present in air, soil and water systems and even at low concentrations is known to cause health risks to animals and

humans [3-7]. Even at blood levels as low as 50 µg/L, research has shown that Pb can damage the infant brain leading to sometimes life-long health problems [8].

Exposure to Pb can occur via many physiological pathways including ingestion, inhalation, or skin contact and can be present in air, food and water [9,10]. For general populations a main source of Pb exposure is through drinking water leading the World Health Organization (WHO) to set a guideline for 10 µg/L in drinking water [11]. These examples undoubtedly demonstrate the importance of Pb pollution control and detection within water bodies and drinking water whilst validating the importance of sensitive heavy metal detection techniques.

The most commonly used analytical techniques for Pb trace and ultra-trace analysis of heavy metals includes potentiometry, voltammetry, and atomic spectrometry, including ICP-AES and ICP-MS [12]. These methods can be time consuming and expensive – especially with ICP techniques. Therefore, cheaper and less time consuming methods are being sought after. Additional problems encountered in determining the concentration of Pb in water are matrix effects and concentrations of Pb lower than the detection limits of standard instrumental methods. These problems can be solved by using a preconcentration/separation method. Standard preconcentration/separation procedures include liquid–liquid extraction, solid-phase extraction, co-precipitation, cloud point extraction and ion-exchange separation. These can limit matrix effects and improve the sensitivity of the analysis method by removing the metal ions from matrices and concentrating the ions via preconcentration[13].

Nanomaterials are now widely integrated into the area of chemical sensors [14, 15]. The success of nanomaterials for sensing applications is due to their distinctive chemical and physical properties that they can possess due to their composition and size which might not be evident in the corresponding bulk material. Novel effects can include a high surface area to volume ratio, light absorption, conductivity, magnetism, mechanical strength, and visible photon emission that can be applied to sensing practices [16-21]. Gold exhibits unique optical properties when fabricated with nanometre dimensions. They exhibit an intense absorption in the visible/near-UV region that is absent in the spectrum of the bulk material. This is a result of the coherent oscillation of the conduction electrons confined to the nanodimensions of the nanomaterial's surface [22]. This is known as localized surface plasmon resonance (LSPR) and is accredited to many of the phenomena that can be induced when using noble metal nanoparticles. These include fluorescence boosting by plasmon enhancement, plasmon quenching and surface enhanced Raman spectroscopy (SERS) which have been developed into analytical methods for the sensing and analysis of chemicals pertaining to heavy metal pollution [23-27].

SERS can be understood as the combination of an electromagnetic enhancement mechanism and a chemical enhancement mechanism. On inducing the LSPR of a nanoparticle surface the local electromagnetic field is enhanced enhancing the Raman scattering signal by an approximate order of 10^4 [28]. Charge-transfer resonances from the metal NP to the surface molecules have also been observed with a chemical enhancement factor of 10^2 arising from the excitation of the surface molecule's localised electronic resonances. This has led to Raman scattering enhancement factors in the

10^4 – 10^{15} range depending on the method employed [29]. Some of the higher enhancement factors can be reached by the production of Raman ‘hotspots’. Causing NP aggregation or closely packed NP arrays produce large electromagnetic fields between neighbouring NPs. This has been demonstrated to improve the signal of SERS spectra by 10^{14} greater than normal Raman signals[48,49].

AuNPs can be functionalised with molecules to capture target chemicals and allow them to build up around the nanoparticles’ surfaces for the purposes of SERS. This means that very weak Raman signals can then be observed of the target chemical. SERS is a dominant nano-analytical method producing impressive limits of detection and has been used to detect ions down to pM concentrations. Remarkably, Silver nanoparticles co-functionalized with cysteine and 3,5-Dimethoxy-4-(6'-azobenzotriazolyl)phenol have been used to detect pM concentrations of Cu^{2+} and Hg^{2+} metal ions via a SERS analytical technique via an aggregation-induced SERS [30]. Also, 2-mercaptoisonicotinic acid (2MNA)-modified AuNPs have also been utilized for the detection of Pb^{2+} ions to 100 nM concentrations in solutions by using chemicals to mask the interactions of other metal ions in the solution [31].

To achieve sensitivity towards metal ions the functionalising molecules on the particles’ surfaces should have a strong affinity for heavy metal ions. The citrate reduction of gold chloride (HAuCl_4) is one of the mostly widely used methods for the preparation of water soluble AuNPs. The citrate molecules are used to stabilise and control the growth and size of the NPs [32-36]. Citrate molecules have a hydroxyl and a carboxyl functional group on the 3rd carbon and a further two terminal carboxyl groups on a pentane back-bone. The carboxyl and hydroxyl groups of the citrate molecules

have a strong affinity to a variety of divalent metal ions including the heavy metals Pb^{2+} , Ni^{2+} , Cd^{2+} and Hg^{2+} [37-40]. This has also been seen when using citrate functionalised AuNPs in some metal solutions [41, 42]. This has brought about several citrate functionalised nanosensors derived from AuNPs [43].

Low maintenance and running costs relative to many low detection limit analytical instruments mean that Raman spectrometers coupled with SERS techniques are much cheaper analysis method than many standard analytical methods with low limits of detection. In this study we have derived a method for determining Pb^{2+} ions at different concentrations designed for after simple separation techniques to cut-out the need for expensive analytical equipment. It is hoped that this will provide a reliable, cheap, and easy-to-use alternative to analytical techniques already employed for the trace and ultra-trace analysis of metals in water.

2. EXPERIMENTAL SECTION

2.1. Chemicals and Materials

Gold(III) chloride trihydrate and trisodium citrate dehydrate, $\text{Pb}(\text{NO}_3)_2$ (ASC >99.0%) CdCl_2 (Technical Grade), NiCl_2 (98%), HgCl_2 (99.5%) and FeCl_2 (98%) were obtained from Sigma-Aldrich, UK.

2.2. Methods

AuNPs were prepared by the standard Turkevich method, which involves reduction of gold chloride using sodium citrate [40]. Water (105 mL) was heated to boiling in a 250 mL conical flask. The water was removed from the heat and trisodium citrate (61.7 mg)

was added. Aqueous $\text{HAuCl}_4 \cdot 3\text{H}_2\text{O}$ (1 mL, 9.9 mg) solution was then added to the citrate solution and left for 15 min whilst stirring. Metal ions stock solutions were prepared for Pb^{2+} , Cd^{2+} , Ni^{2+} , Hg^{2+} and Fe^{2+} (3.81×10^{-4} M) and diluted to concentrations ranging from (3.81×10^{-4} M – 5.18×10^{-6} M). Metal ion solutions were then added to the AuNP solutions as a 1 to 1 volume ratio. SERS samples were prepared by dropping 60 μL of AuNPs solution or metal ion/AuNPs mixtures onto glass slides and drying in an oven at 70°C . The metal ion/AuNP solutions were dried onto glass slides to create a closely packed AuNP array to encourage Raman hotspots to further enhance the SERS signal. For the assessment of the sensing capabilities of this SERS based method, the concentration of Pb^{2+} ions will be noted in the ng/L units which is standard notation for metal concentrations in water systems.

2.3 Characterisation

UV-Vis absorption spectroscopy was carried out to determine the LSPR absorption maximums of the AuNPs and metal ion/AuNPs solutions (Perkin Elmer Lambda 40 UV-Vis Spectrometer). Analysis of the size and morphology of the AuNPs was performed using transmission electron microscopy (TEM, Philips Technai 12 Biotwin) and photon correlation spectroscopy (PCS, Zetasizer Nano ZS, Malvern Instrument, UK).

Attenuated total reflectance Fourier transform infrared (ATR-FTIR, Thermoscientific Nicolet iS5 FTIR iD5 ATR) spectroscopy was used to obtain vibrational spectra of the surface citrate and metal citrate species present on the AuNPs surfaces. Solutions were added to glass slides by dropping a single drop from a graduated glass pipette (20 μL) and allowing the sample to dry in air. A blank ATR-FTIR sample spectrum was obtained

for a clean glass slide and then the spectra were recorded for the AuNPs and metal ion/AuNPs solutions. SERS spectroscopy was used to obtain vibrational spectra of the citrate functional molecules on the AuNPs surfaces before and after the addition of different concentrations of metal ions (Renishaw inVia Raman Microscope with a 514 nm argon laser, 50 mW).

3. RESULTS AND DISCUSSION

3.1 Mechanistic basis for the system

The transmission electron microscopy micrograph confirms the synthesis of monodispersed AuNPs (Figure 1). The AuNPs exhibited LSPR, as shown by the deep red solution and a single LSPR absorbance band in the absorption spectrum, characteristic of non-aggregated solutions (Figure 1 insert). The synthesised citrate functionalised AuNPs were shown to be ca. 6 nm in diameter and well dispersed with a surface charge of -44.3 mV, indicating a stable colloidal solution, according to DLVO theory[45,46].

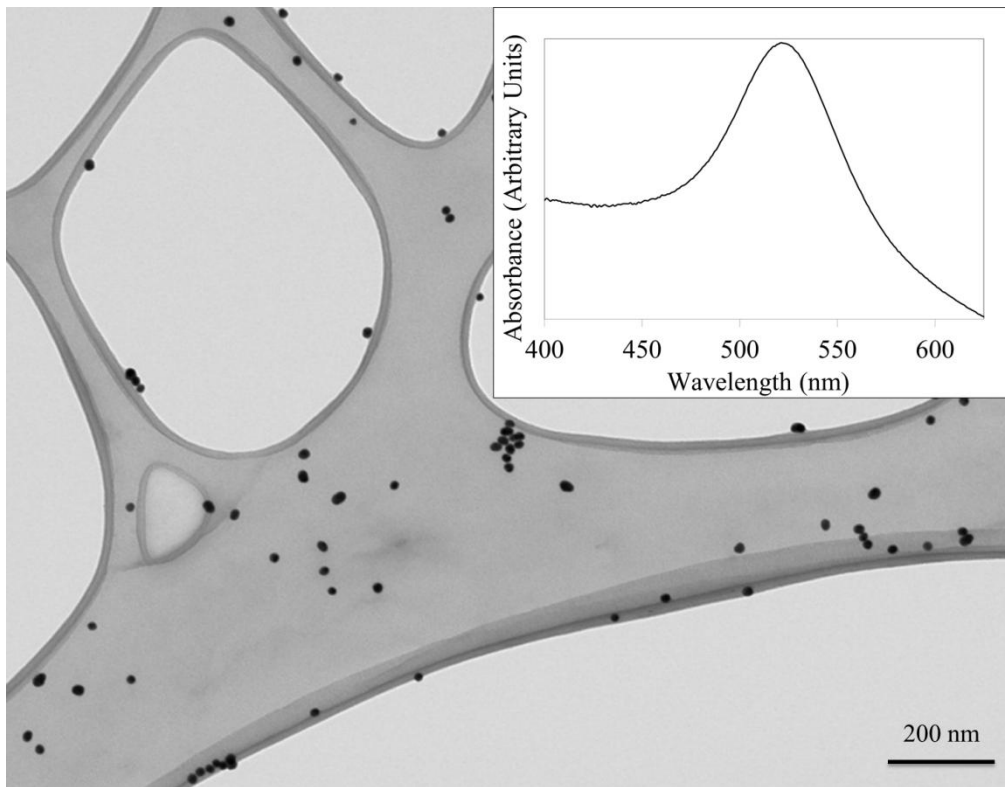


Figure 1. TEM micrograph of the c.a. 6 nm diameter, well dispersed AuNPs used here. (Insert) The absorption spectrum for the citrate functionalised AuNPs synthesised here.

In the presence of a 0.19 mM concentration of Pb^{2+} ions the AuNPs underwent rapid aggregation resulting in a blue solution, which became clear after 15 minutes. This a result of the broadening of the LSPR absorption band, which is attributed to the effects of plasmon coupling, experienced when plasmonic NPs come into close proximity (Figure 2 insert)[47].

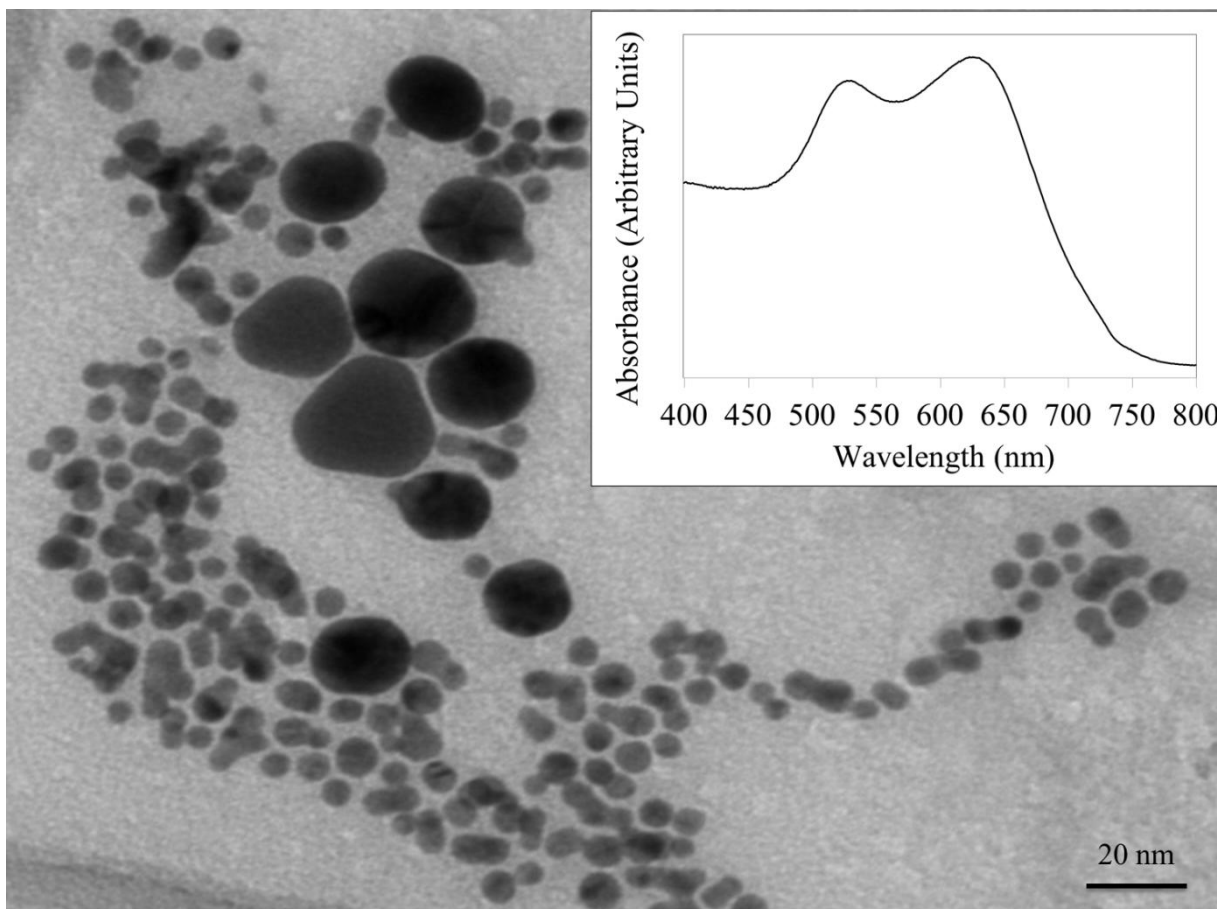


Figure 2. TEM of aggregated AuNPs, after the addition of presence of Pb^{2+} ions (0.19 mM), and the corresponding UV-Vis absorption spectrum for the same aggregated AuNP solution.

As a comparison to Pb^{2+} ions, Ni^{2+} , Cd^{2+} , and Hg^{2+} ions (0.19 mM) were added to different AuNP solutions. These samples displayed no features of plasmon coupling in the UV-Vis absorption spectra and the solutions remained relatively red. Although, the addition of the Ni^{2+} , Cd^{2+} , and Hg^{2+} ions did produce relatively minor LSPR absorption band shifts of -18 nm to +30 nm, indicating that the metal ions were interacting with the citrate molecules bound to the surfaces of the AuNPs.

3.2 SERS spectra of citrate functionalised AuNPs.

Figure 3 shows a SERS spectrum for the citrate molecules bound to the surface of the AuNPs. The bands situated at 1578 cm^{-1} and 1373 cm^{-1} are respectively due to the asymmetric and symmetric stretches of the carboxylate groups ($\nu_{\text{as}}(\text{COO}^-)$ and $\nu_{\text{s}}(\text{COO}^-)$). The symmetric stretch band of the carboxylate has shifted from the literature value for free citrate molecules (1417 cm^{-1}), which reveals that the citrate molecules had adsorbed onto the surfaces of the AuNPs[50]. In addition to the carboxylate group stretching modes, there are the bands assigned to the stretching modes of the citrate hydroxyl group, located at 1096 cm^{-1} ($\nu(\text{C-OH})$) and $\sim 3200\text{ cm}^{-1}$ ($\nu(\text{O-H})$).

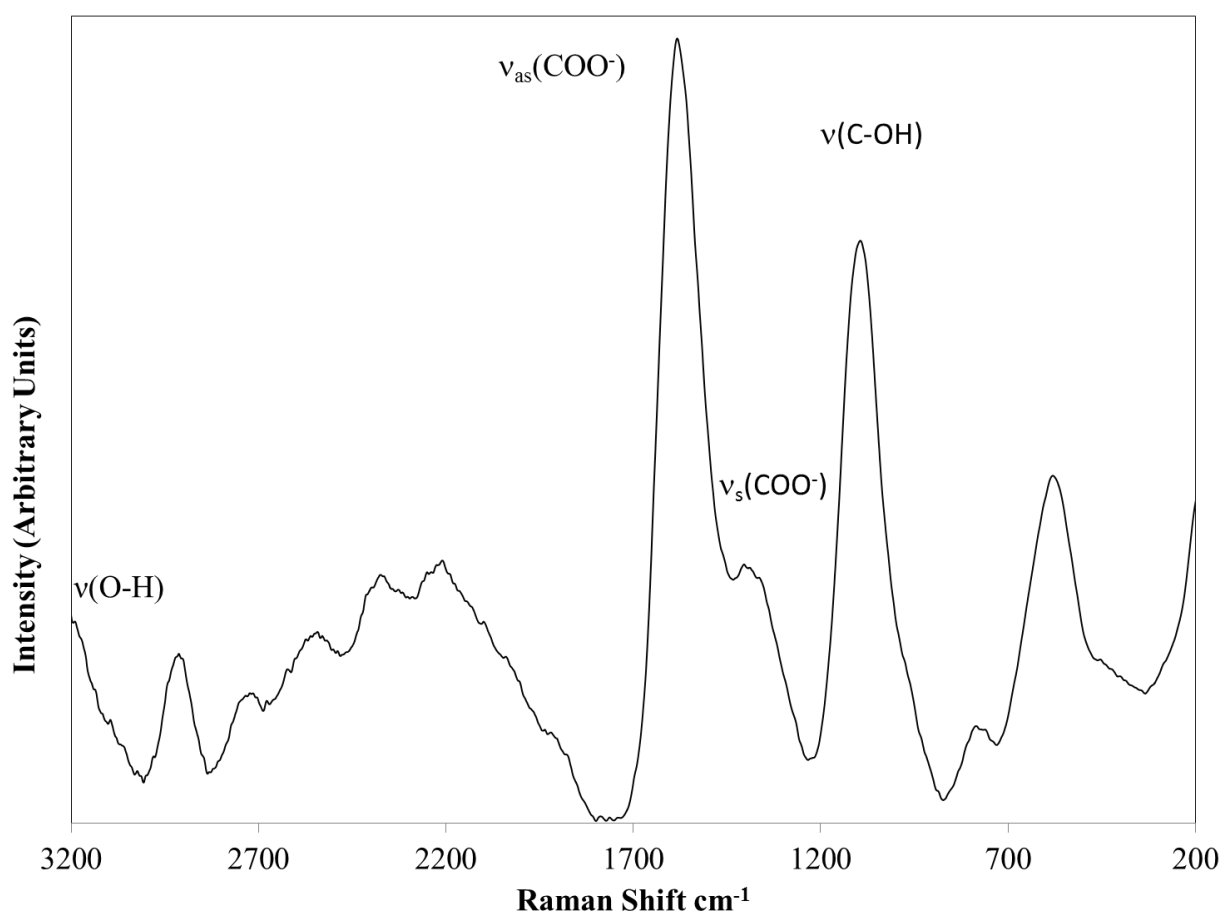


Figure 3. SERS of the surface citrate molecules functionalising AuNPs

3.3 Effect of Pb^{2+} ion interactions with the surface citrates.

The interaction between the carboxylate groups of the surface-bound citrate molecules with the Pb^{2+} ions was evident as the intensities of the $\nu_{as}(COO^-)$ and $\nu_s(COO^-)$ bands were altered (Figure 4). A noteworthy feature of the spectrum is that the $\nu(O-H)$ Raman band has reduced considerably. When comparing ATR-FTIR spectra for the AuNP and $Pb^{2+}/AuNP$ SERS samples, it is evident that the $\nu(O-H)$ band reduced on the addition of Pb^{2+} ions (Figure 5). These changes to the $\nu(O-H)$ band were directly dependent on the concentration of the Pb^{2+} ions in the AuNP solution. In addition, the pH value was inversely proportional to the concentration of the Pb^{2+} ions, suggesting the loss of the $\nu(O-H)$ band is a result of the de-protonation of the hydroxyl group upon Pb^{2+} binding.

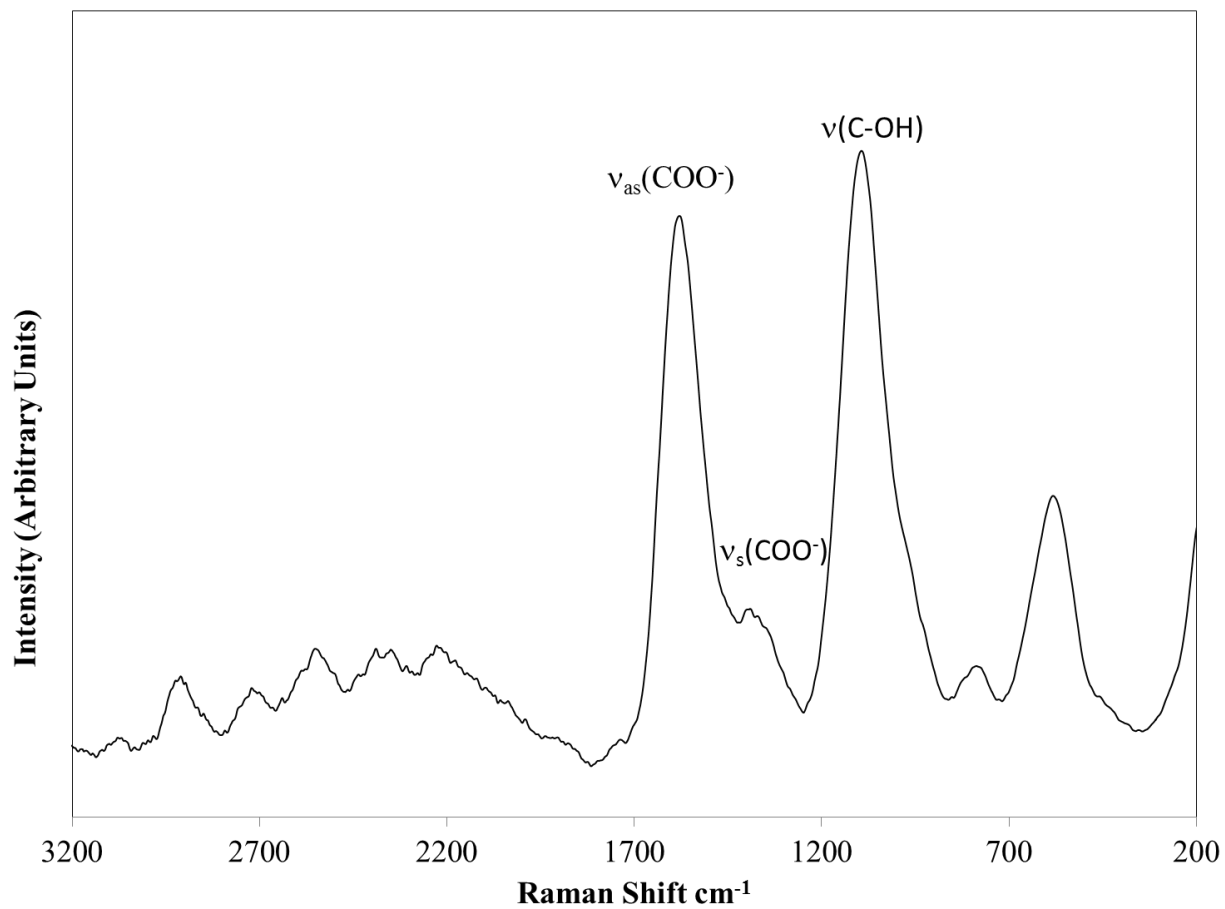


Figure 4. SERS spectrum for the Pb²⁺/AuNP sample (0.19 mM)

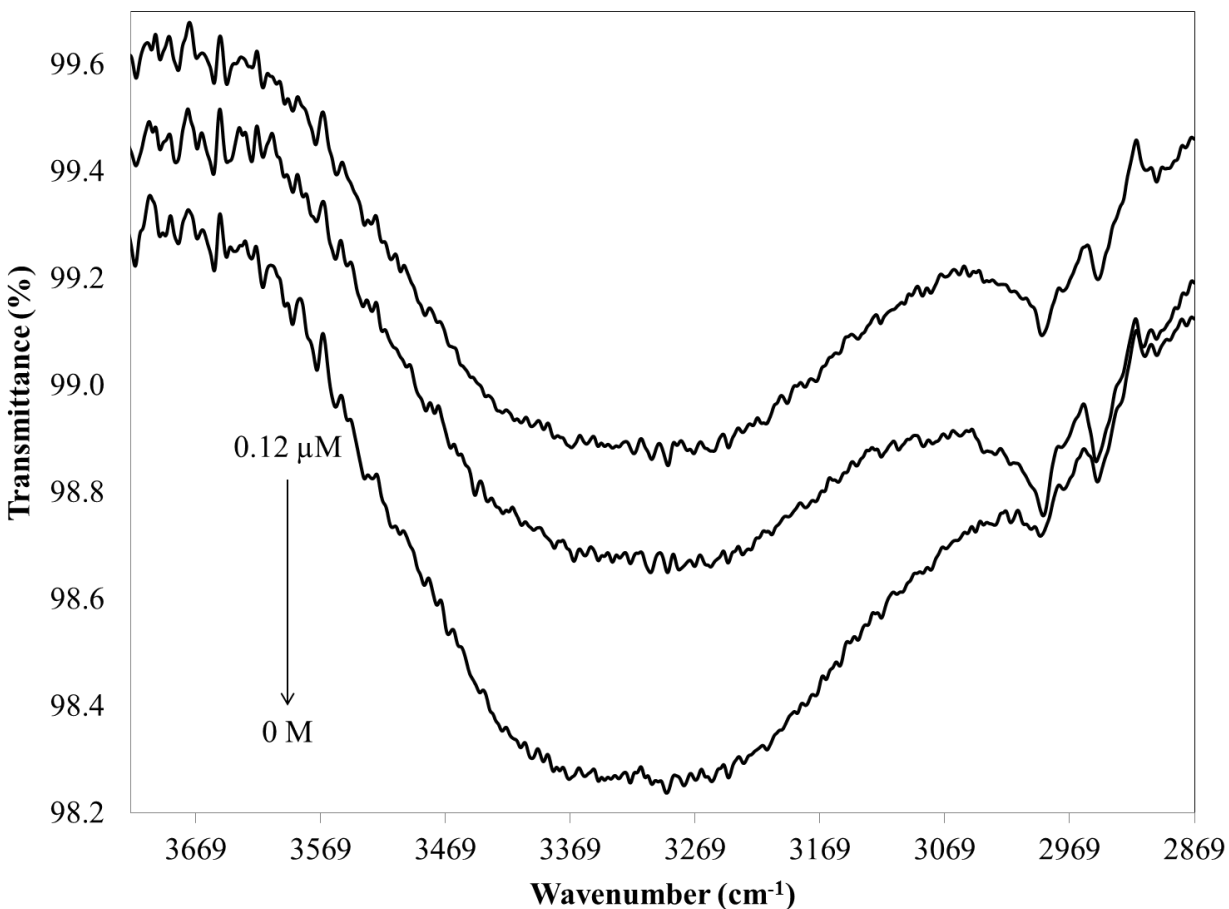


Figure 5. ATR-FTIR spectrum for the hydroxyl group of the Pb²⁺/AuNP samples with difference concentrations of Pb²⁺ ions

Ni²⁺, Cd²⁺, and Hg²⁺ ions also altered the $\nu_{as}(\text{COO}^-)$ and $\nu_s(\text{COO}^-)$ Raman bands indicating the binding of the ions with the functional molecule's carboxylate groups. The SERS spectra obtained for each the metal ion/AuNP sample was different with respects to the $\nu_{as}(\text{COO}^-)$ and $\nu_s(\text{COO}^-)$ band positions and intensity. Additionally, in comparison to the Pb²⁺/AuNP sample all of the other metal ions retained their $\nu(\text{O-H})$ band. Although these spectra were noticeably different it was impossible to determine a

preferred metal-citrate species from a mixed metal ion solution containing 0.19 mM of Ni^{2+} , Cd^{2+} , Pb^{2+} and Hg^{2+} ions (Figure 8).

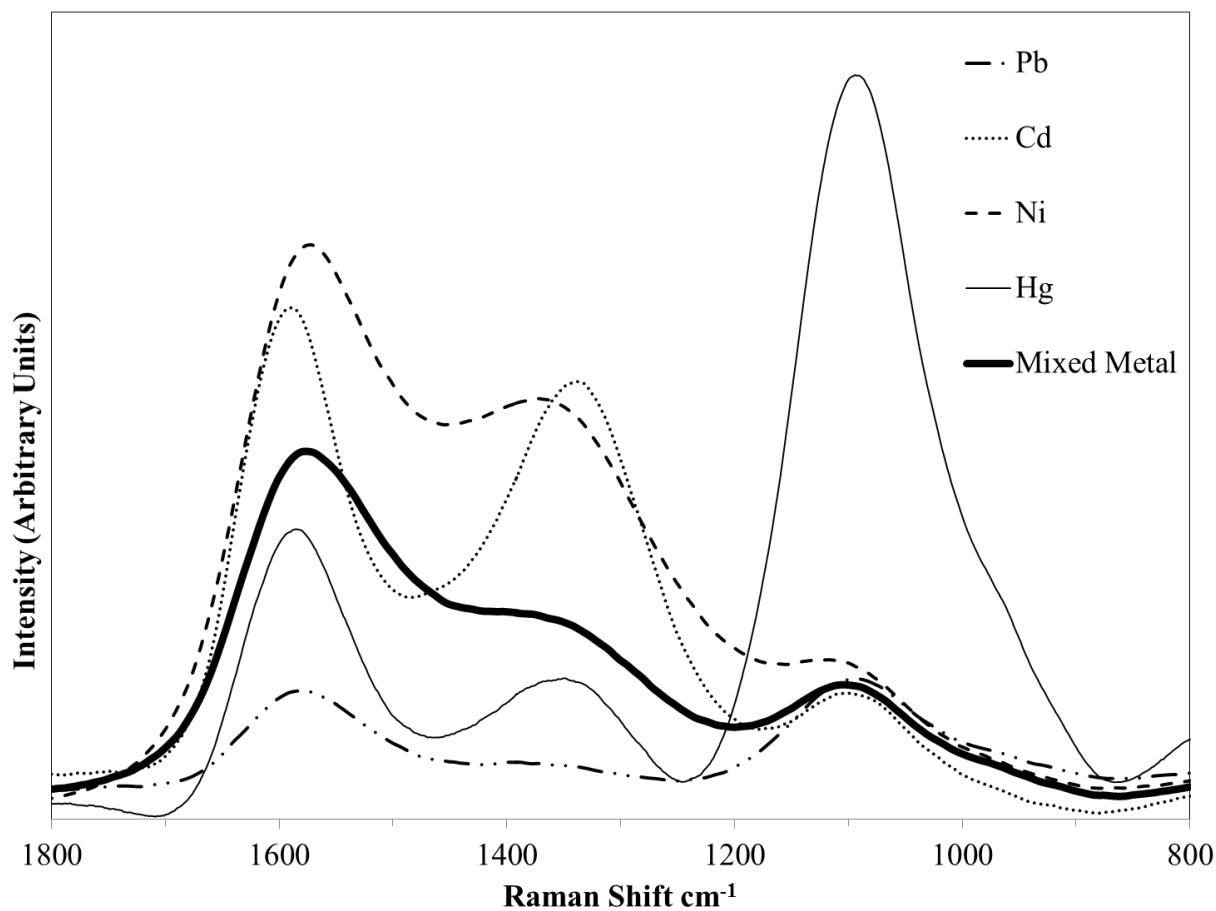


Figure 6. SERS spectra for the $\nu_{\text{as}}(\text{COO}^-)$ and $\nu_{\text{s}}(\text{COO}^-)$ Raman bands for the Ni^{2+} , Cd^{2+} , Pb^{2+} and Hg^{2+} ion/AuNP samples (0.19 μM) and a mixed metal ion/AuNP solution containing all of the above metal ions (0.19 μM)

3.4 Effect of the Concentration of Pb^{2+} and the sensitivity of the SERS Sensor.

As the concentrations increase from 0 to 1000 ng/L the intensities of the $\nu_{\text{as}}(\text{COO}^-)$ and $\nu_{\text{s}}(\text{COO}^-)$ bands decreased and then increased again at 25 ng/L (Figure 7).

Contrastingly, the $\nu(\text{C-OH})$ band decreased on decreasing the Pb^{2+} ion concentration. For the peak intensity for $\nu(\text{C-OH})$ there is a deviation from linearity when the concentration of Pb^{2+} is lowered to <25 ng/L. The fact that at 25 ng/L the $\nu_{\text{as}}(\text{COO}^-)$ and $\nu_{\text{s}}(\text{COO}^-)$ bands increase in intensity and the $\nu(\text{O-H})$ band re-appears would indicate a different metal citrate species being formed at concentrations <25 ng/L than the metal citrate species being formed >25 ng/L. This change in metal citrate bonds, though unpredicted, can be expected, as the metal to citrate ratio is an important factor in which metal-citrate species are formed.

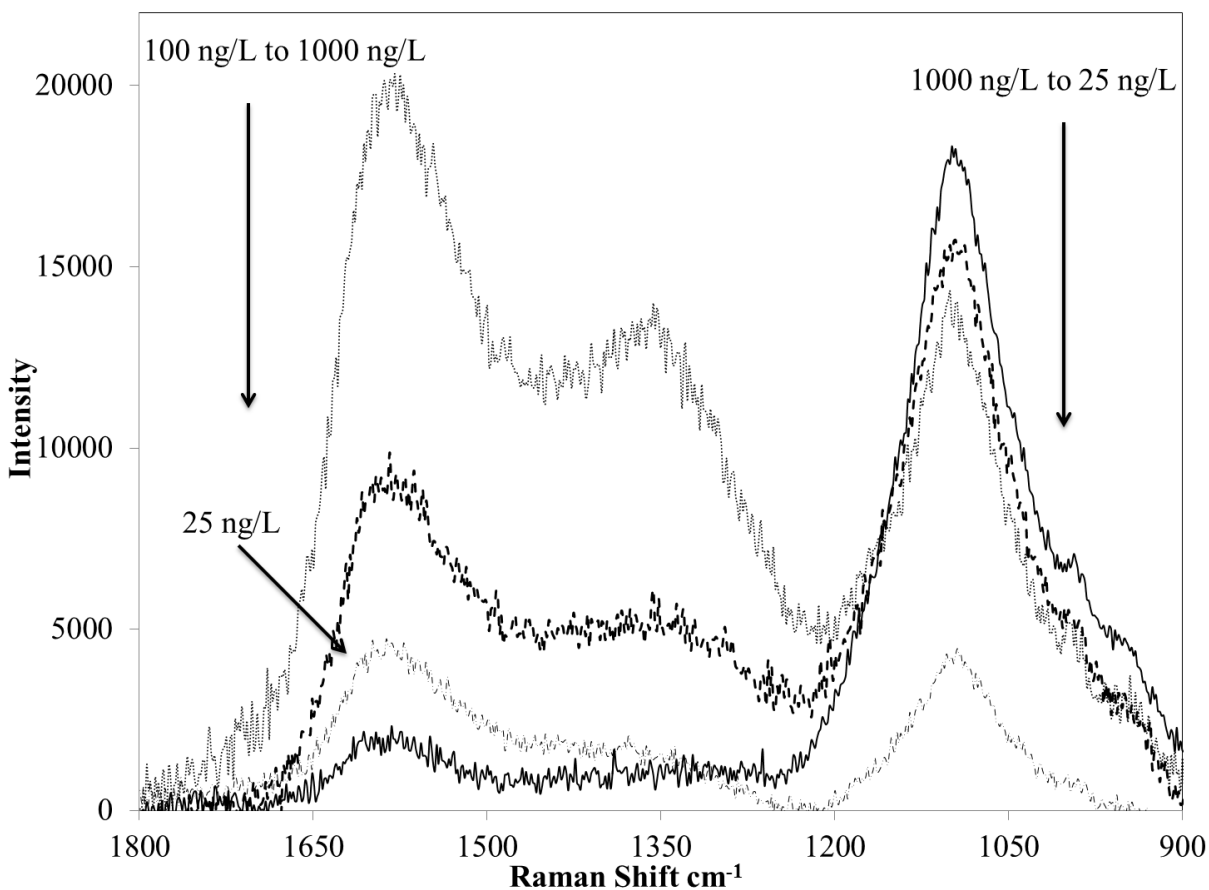


Figure 7. SERS spectra for the $\nu_{as}(\text{COO}^-)$ and $\nu_s(\text{COO}^-)$ Raman bands for the Pb^{2+} ion/AuNP samples

The SERS spectral readings were repeated five times and the peak heights for the $\nu(\text{C-OH})$ band were averaged with an average standard deviation (SD) of 2.057 and an average relative standard deviation (RSD) of 0.147%. Taking the ratio between the averaged peak heights for the $\nu(\text{C-OH})$ band for the AuNP solution and the Pb^{2+} /AuNPs ($I_0/n(\nu(\text{C-OH}))$) and plotting it against the concentration of Pb^{2+} ions produced a linear fit ($R^2 = 0.9982$) between 50 ng/l and 1000 ng/l (Figure 8).

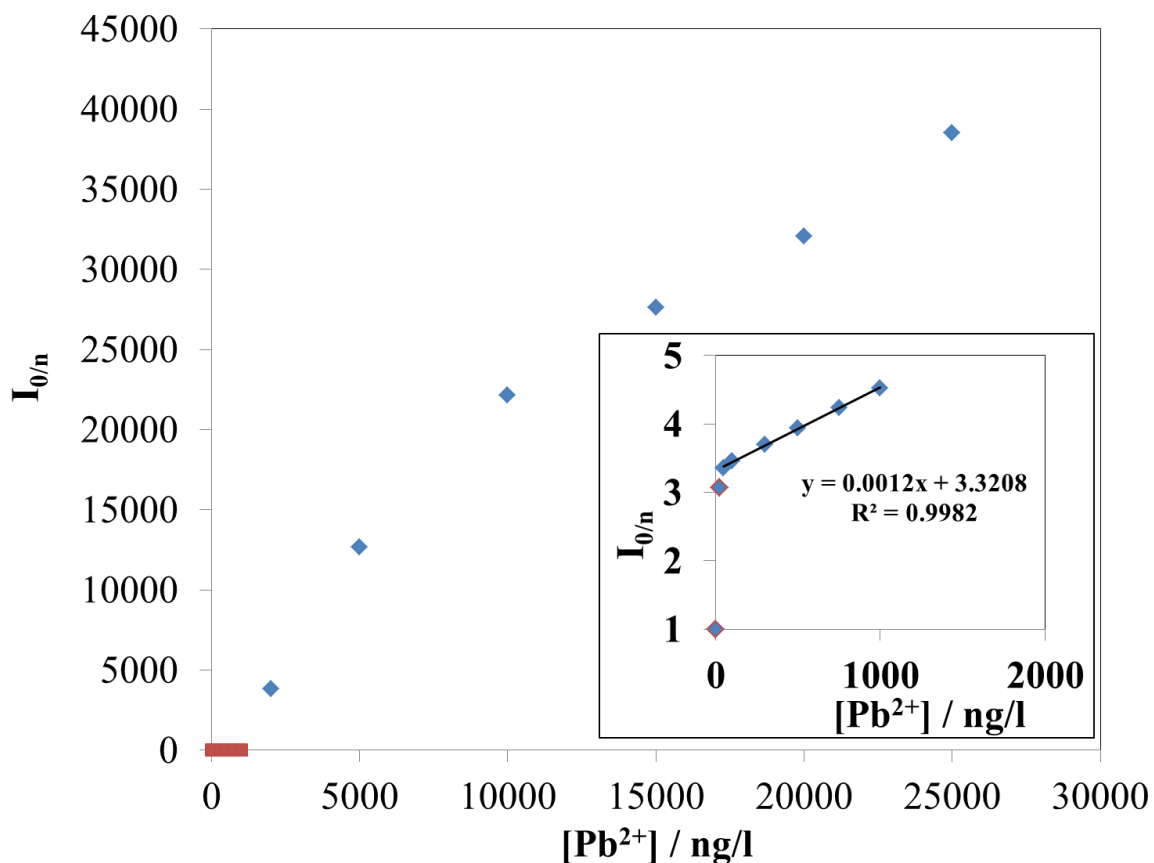


Figure 8. Ratio between the averaged peak heights for the $\nu(\text{C-OH})$ band for the AuNP solution and the $\text{Pb}^{2+}/\text{AuNPs}$ over a Pb^{2+} ion concentration range of 0 to 25000 ng/L produced a linear fit between 50 ng/l to 1000 ng/l (Insert).

A plot of $(I_0/n(\nu(\text{C-OH})))$ against the concentration of Pb^{2+} ions for concentrations 1000 ng/l to 25000 ng/l produced a polynomial fit ($n = 3$) with an R^2 value of 1 (Figure 9).

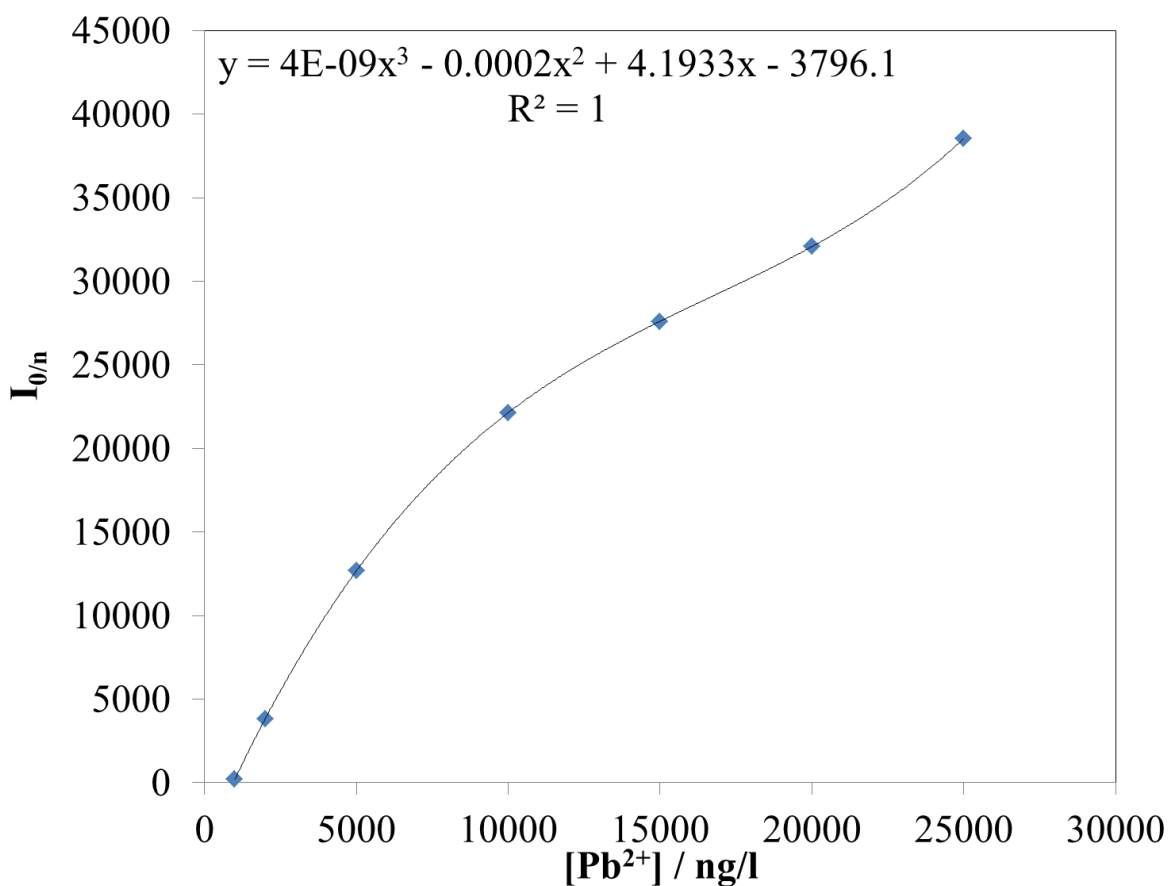


Figure 9. A plot of $(I_0/n(\nu(\text{C-OH})))$ against the concentration of Pb^{2+} ions for concentrations 1000 ng/l to 25000 ng/l

3.5 Considerations for practical use.

A solution of Pb^{2+} ions was determined to be 10680 ng/l by ICP-AES. This was determined to be 10000 ng/l by this SERS based technique. Due to the low limit of detection for the AuNP SERS analysis method the Pb^{2+} solution was then diluted by 1 in 100. Using the SERS analytical approach developed here, the solution was determined to be 100 ng/l. Both measurements displayed a 98.6% recovery with a RSD of 2.1% ($n = 5$), which shows that this method is competitive with current preconcentration techniques coupled with analytical methods (Table 1). As this SERS technique is non-ion specific, replacing the spectroscopy component (GFAAS or FAAS) with this SERS technique and retaining the preconcentration step to obtain selectivity could yield very high limits of detection (LOD) but at a much lower cost.

Table 1 Real water sample determination of Pb^{2+} using preconcentration steps

Preconcentration Method	% Recovery	LOD	RSD (%)	Ref
Cloud-point extraction	104 – 98.6	1100 ng/L (FAAS)	3.5 for 20 $\mu\text{g/L}$	(51)
Cloud-point extraction	104 – 97.8	80 ng/L (GFAAS)	2.8 for 5 $\mu\text{g/L}$	(52)
Solid-phase extraction	95.3 – 97.4	610 ng/L (FAAS)	3.56 for 20 $\mu\text{g/L}$	(53)

4.0. CONCLUSIONS

In the present work, we have successfully demonstrated a highly sensitive SERS method for the detection of Pb^{2+} ions in aqueous media. The experimental results showed that Pb^{2+} ions could be detected accurately with a high sensitivity (LOD 25 ng/L) over a wide linear range (25 ng/L – 1000 ng/L). Due to the non-selective nature, this technique would be highly useful for post-preconcentration steps, where Pb^{2+} ions are the only metal ions in the analyte solution. A major advantage for this technique is that Raman spectrometers are relatively cheaper to purchase and maintain than many standard analytical techniques (ICP-AES, FAAS, GFAAS). Thus, a preconcentration/SERS technique would provide high limits of detection, high sensitivity and a cheaper analysis cost giving this cost-effective and sensitive sensing system great potential for practical application.

ACKNOWLEDGMENTS

This research was funded by the Dalton Research institute and United Utilities.

REFERENCES

1. Xie, X., Ding, G., Cui, C., Chen, L., Gao, Y., Zhou, Y., Tian, Y. *Environmental Pollution*, 175, (2013), 30-34.
2. Needleman, H. Lead poisoning. *Annu. Rev. Med.* 55 (2004) 209-222.
3. Gamiño-Gutiérrez, S. P., González-Pérez, C. I., Gonsebatt, M. E., & Monroy-Fernández, M. G. *Environmental geochemistry and health*, 35 (2013) 37-51.
4. Hou, S., Yuan, L., Jin, P., Ding, B., Qin, N., Li, L. & Deng, Y. *Theoretical Biology and Medical Modelling*. 10 (2013) 1-9.
5. Neal, A. P., & Guilarte, T. R. *Toxicology Research*. 2 (2013) 99-114.

6. Xie, X., Ding, G., Cui, C., Chen, L., Gao, Y., Zhou, Y. Tian, Y. *Environmental Pollution*. 175 (2013) 30-34.
7. Authman, M. M., Ibrahim, S. A., El-Kasheif, M. A., & Gaber, H. S. *Global Veterinaria* 10 (2013) 103-115.
8. Lanphear, B. P., Dietrich, K., Auinger, P., & Cox, C. *Public health reports*. 115 (2000) 521.
9. Papanikolaou, N. C., Hatzidaki, E. G., Belivanis, S., Tzanakakis, G. N., & Tsatsakis, A. M. *Medical science monitor*. 11 (2005) 329.
10. USEPA Lead compounds hazard summary (2000)
11. World Health Organization (WHO) Guidelines for drinking water quality, second edition. Recommendations. Geneva (2004) vol 1
12. Brown, R. J., & Milton, M. J. *TrAC Trends in Analytical Chemistry*. 24 (2005) 266-274.
13. Alothman, Z. A., Yilmaz, E., Habila, M., Shabaka, A., & Soylak, M. *Microchimica Acta*. (2013) 1-6. DOI: 10.1007/s00604-013-0979-6
14. Zhang, L., & Fang, M. *Nano Today*. 5 (2010) 128-142
15. Choi, I., & Choi, Y. *IEEE Journal of Selected Topics in Quantum Electronics*. 18 (2012) 1110-1121.
16. Riu, J.; Maroto, A.; Rius, F. X. *Talanta*. 69 (2006) 288-301.
17. Lupan, O.; Chai, G.; Chow, L. *Microelectronic Engineering*. 85 (2008) 2220-2225.
18. Sperling, R. A.; Parak, W. J. *Philosophical Transactions of the Royal Society A: Mathematical, Physical and Engineering Sciences*. 368 (2010) 1333-1383.

19. Mu, L.; Shi, W.; Chang, J. C.; Lee, S. T. *Nano letters*. 8 (2008) 104-109.
20. Frigoli, M.; Ouadahi, K.; Larpent, C. A. *Chemistry-A European Journal*. 15 (2009) 8319-8330.
21. Li, H.; Li, Y.; Cheng, J. *Chemistry of Materials*, , 22 (2010) 2451-2457.
22. Moores, A.; Goettmann, F. *New J. Chem.*, 30 (2006) 1121-1132.
23. Kern, A. M., Meixner, A. J., & Martin, O. J. *ACS nano*. 6 (2012) 9828-9836.
24. Chen, H., Shao, L., Woo, K. C., Wang, J., & Lin, H. Q. *The Journal of Physical Chemistry C*. 116 (2012) 14088-14095.
25. Choi, I., & Choi, Y. *IEEE Journal of Selected Topics in Quantum Electronics*. 18 (2012) 1110-1121.
26. Anker, J. N., Hall, W. P., Lyandres, O., Shah, N. C., Zhao, J., & Van Duyne, R. P. *Nature materials*. 7 (2008) 442-453.
27. Su, S., Wu, W., Gao, J., Lu, J., & Fan, C. *Journal of Materials Chemistry*. 22 (2012) 18101-18110.
28. Campion, A., & Kambhampati, P. *Chem. Soc. Rev.* 27 (1998) 241-250.
29. Hering, K., Cialla, D., Ackermann, K., Dörfer, T., Möller, R., Schneidewind, H., ... & Popp, J. *Analytical and bioanalytical chemistry*, 390 (2008) 113-124.
30. Li, F., Wang, J., Lai, Y., Wu, C., Sun, S., He, Y., & Ma, H. (2012). *Biosensors and Bioelectronics*. 39 (2013) 82–87.
31. Tan, E., Yin, P., Lang, X., Zhang, H., & Guo, L. *Spectrochimica Acta Part A: Molecular and Biomolecular Spectroscopy*. 97 (2012) 1007–1012.
32. Ji, X.; Song, X., Li, J.; Bai, Y.; Yang, W.; Peng, X. *Journal of the American Chemical Society*, , 129 (2007) 13939-13948.

33. Turkevich, J. Colloidal gold. Part II. Gold Bulletin. 18 (1985) 125-131.
34. Henglein, A.; Giersig, M. The Journal of Physical Chemistry B. 103 (1999) 9533-9539.
35. Pillai, Z. S., & Kamat, P. V. The Journal of Physical Chemistry B. 108 (2004) 945-951.
36. Canamares, M. V.; Garcia-Ramos, J. V.; Gomez-Varga, J. D., Domingo, C.; Sanchez-Cortes, S. Langmuir. 21 (2005) 8546-8553.
37. Koutsoulis, N. P., Giokas, D. L., Vlessidis, A. G., & Tsogas, G. Z. Analytica Chimica Acta. 669 (2010) 45-52.
38. Guan, J., Jiang, L., Zhao, L., Li, J., & Yang, W. Colloids and Surfaces A: Physicochemical and Engineering Aspects. 325 (2008) 194-197.
39. Hidber, P. C., Graule, T. J., & Gauckler, L. J. Citric acid—a dispersant for aqueous alumina suspensions. Journal of the American Ceramic Society. 79 (1996) 1857-1867.
40. Kim, Y., Johnson, R. C., & Hupp, J. T. Gold nanoparticle-based sensing of “spectroscopically silent” heavy metal ions. Nano Letters. 1 (2001) 165-167.
41. Guan, J., Jiang, L., Zhao, L., Li, J., and Yang, W. (2008). Colloids and Surfaces A: Physicochemical and Engineering Aspects, 2008, 325, 194-197.
42. Jiang, L.; Guan, J.; Zhao, L.; Li, J.; Yang, W. Colloids and Surfaces A: Physicochemical and Engineering Aspects, 2009, 346, 216-220.
43. Vilela, D.; González, M. C.; Escarpa, A. Chemical Creativity Behing the Assay. Analytica Chimica Acta. 751 (2012) 24-43.

44. Link, S.; El-Sayed, M. A. *The Journal of Physical Chemistry B*. 103 (1999) 4212-4217.
45. Floate, S., Hosseini, M., Arshadi, M. R., Ritson, D., Young, K. L., & Nichols, R. J. *Journal of Electroanalytical Chemistry*, 542 (2003) 67-74.
46. Diegoli, S., Manciuola, A. L., Begum, S., Jones, I. P., Lead, J. R., & Preece, J. A. *Science of the Total Environment*. 402 (2008) 51-61.
47. Reinhard, B. M., Siu, M., Agarwal, H., Alivisatos, A. P., & Liphardt, J. *Nano Letters*. 5 (2005) 2246-2252.
48. Chen, G., Wang, Y., Yang, M., Xu, J., Goh, S. J., Pan, M., & Chen, H. *Journal of the American Chemical Society*. 132 (2010) 3644-3645.
49. Imura, K., Okamoto, H., Hossain, M. K., & Kitajima, M. Visualization of localized intense optical fields in single gold-nanoparticle assemblies and ultrasensitive Raman active sites. *Nano letters*. 6 (2006) 2173-2176.
50. Munro, C. H., Smith, W. E., Garner, M., Clarkson, J. W. P. C., & White, P. C. *Langmuir*. 11(1995) 3712-3720.
51. Li, P., Liu, H., Yang, L., & Liu, J. (2013). *Talanta*. 106 (2013) 381–387.
52. Chen, J., & Teo, K. C. *Analytica Chimica Acta*. 450 (2001) 215-222.
53. Chen, J., Xiao, S., Wu, X., Fang, K., & Liu, W. *Talanta*. 67 (2005) 992-996.

FIGURES

Figure 1. TEM image of the AuNPs used here

Figure 2. The extinction spectrum for the AuNPs used here

Figure 3. Some configurations of surface-bound citrate molecules

Figure 4. TEM of aggregated AuNPs after the addition in the presence of Pb^{2+} ions (0.19 mM)

Figure 5. SERS of the surface citrate molecules functionalising AuNPs

Figure 6. SERS spectrum for the Pb^{2+} /AuNP sample (0.19 mM)

Figure 7. ATR-FTIR spectrum for the hydroxyl group of the Pb^{2+} /AuNP samples with difference concentrations of Pb^{2+} ions

Figure 8. SERS spectra for the $\nu_{as}(COO^-)$ and $\nu_s(COO^-)$ Raman bands for the Ni^{2+} , Cd^{2+} , Pb^{2+} and Hg^{2+} ion/AuNP samples (0.19 μ M) and a mixed metal ion/AuNP solution containing all of the above metal ions (0.19 μ M)

Figure 9. SERS spectra for the $\nu_{as}(COO^-)$ and $\nu_s(COO^-)$ Raman bands for the Pb^{2+} ion/AuNP samples

Figure 10. Ratio between the averaged peak heights for the $\nu(C-OH)$ band for the AuNP solution and the Pb^{2+} /AuNPs over a Pb^{2+} ion concentration range of 0 to 1000 ng/L produced a linear fit

TABLES

Table 1 Real water sample determination of Pb^{2+} using preconcentration steps

Preconcentration Method	% Recovery	LOD	RSD (%)	Ref
Cloud-point extraction	104 – 98.6	1100 ng/L (FAAS))	3.5 for 20 μ g/L	(51)
Cloud-point extraction	104 – 97.8	80 ng/L (GFAAS)	2.8 for 5 μ g/L	(52)

Solid-phase extraction	95.3 – 97.4	610 ng/L (FAAS)	3.56 for 20 (53) µg/L
------------------------	-------------	-----------------	--------------------------

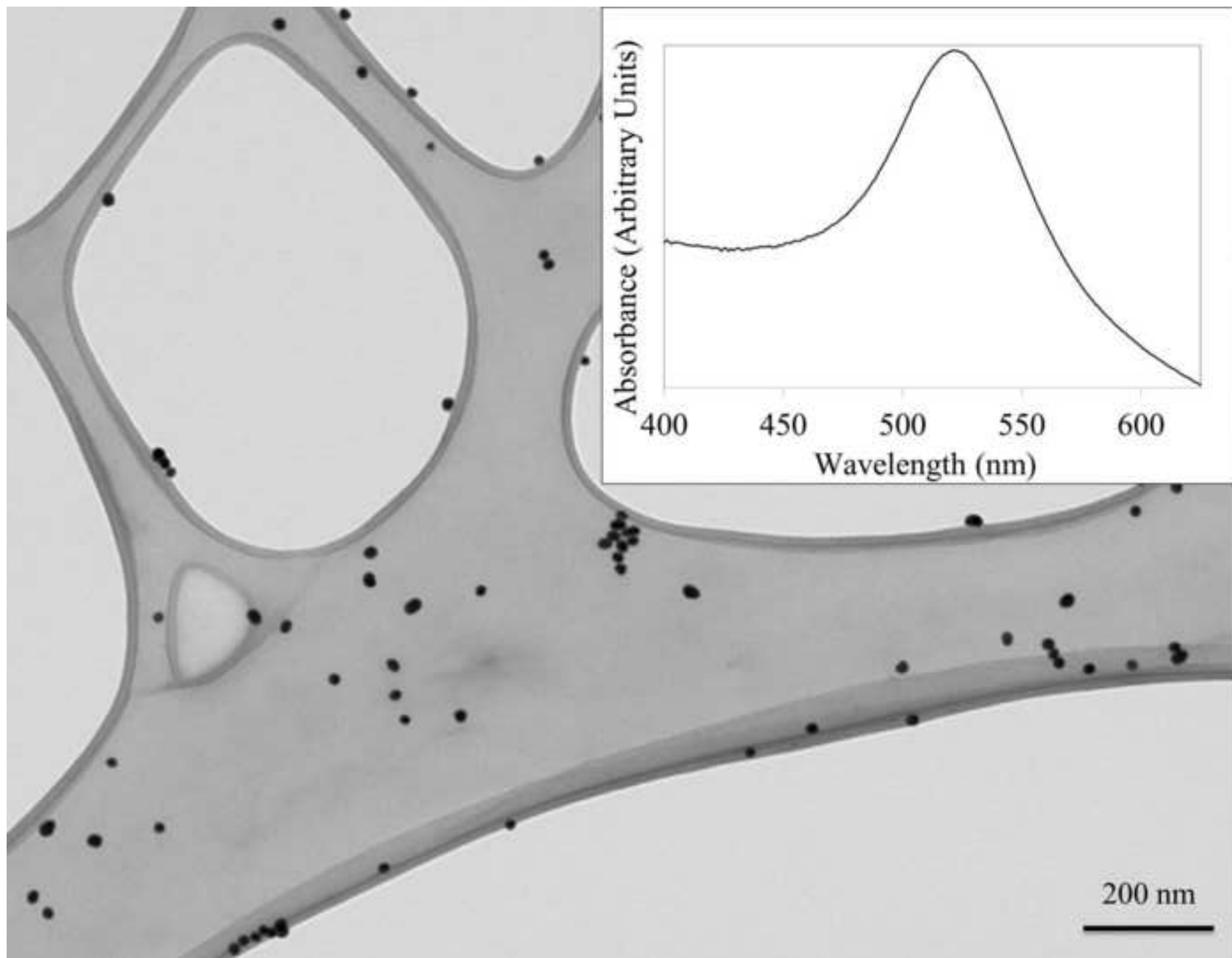
BIOGRAPHIES:

Mark Frost is now studying for his PhD at Manchester Metropolitan University with a research interest covering the production of nanosensors for the detection of chemical pollutants in water.

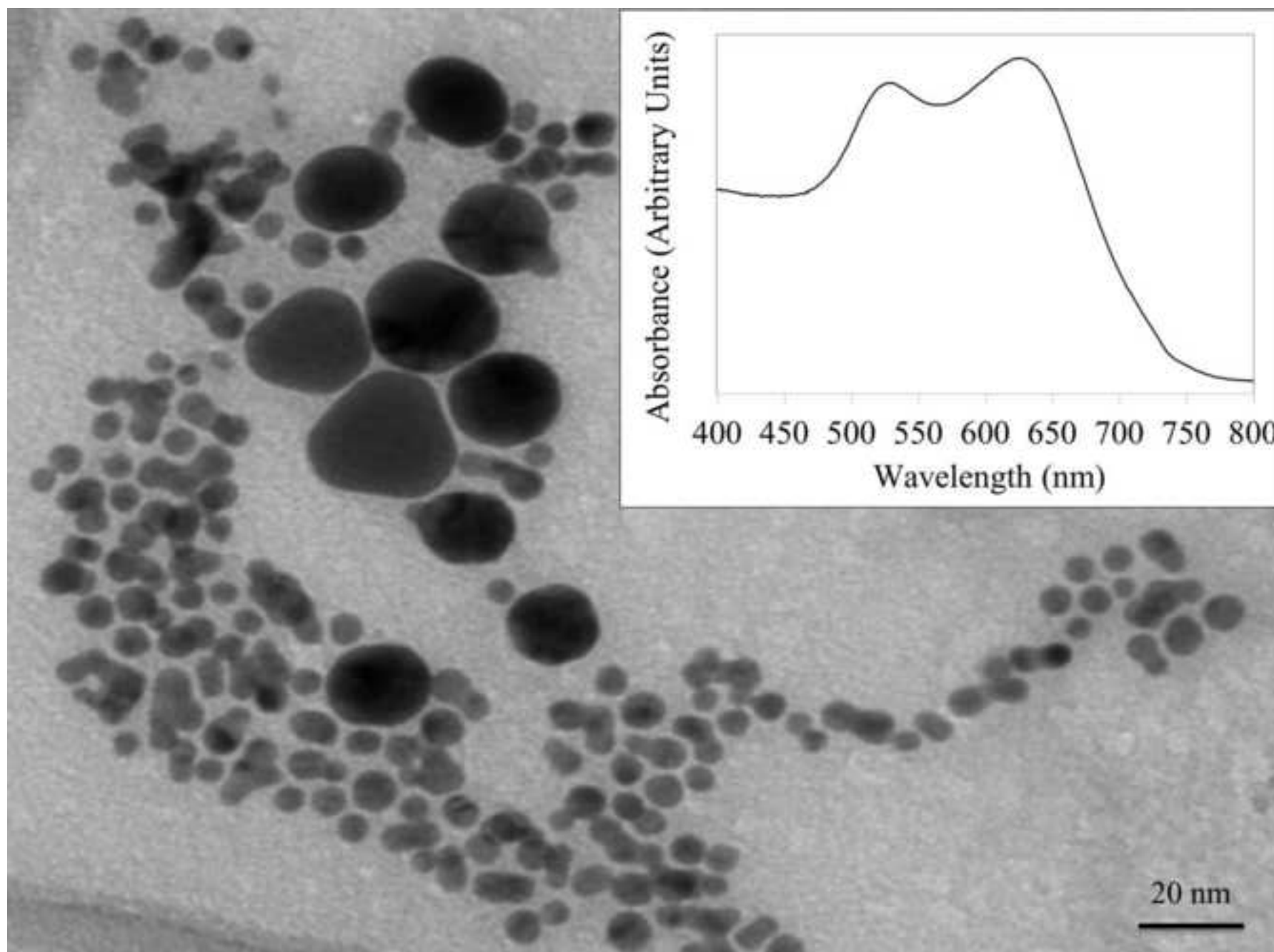
Mike Dempsey is an applied microbiologist with an interest in water and wastewater treatment. Inventor of improvements to expanded and fluidized bed biofilm reactor technology. He is also the Head of Faculty Research Degrees and Head of Faculty Centre for Postgraduate and Early Career Researchers.

Debra Whitehead is a senior Lecturer at the School of Science and the Environment at Manchester Metropolitan University. She leads a advanced functional nanoparticle group and has research interests in creating multifunctional nanoparticles for applications in particle toxicity, water pollutant detection and targeted slow drug release

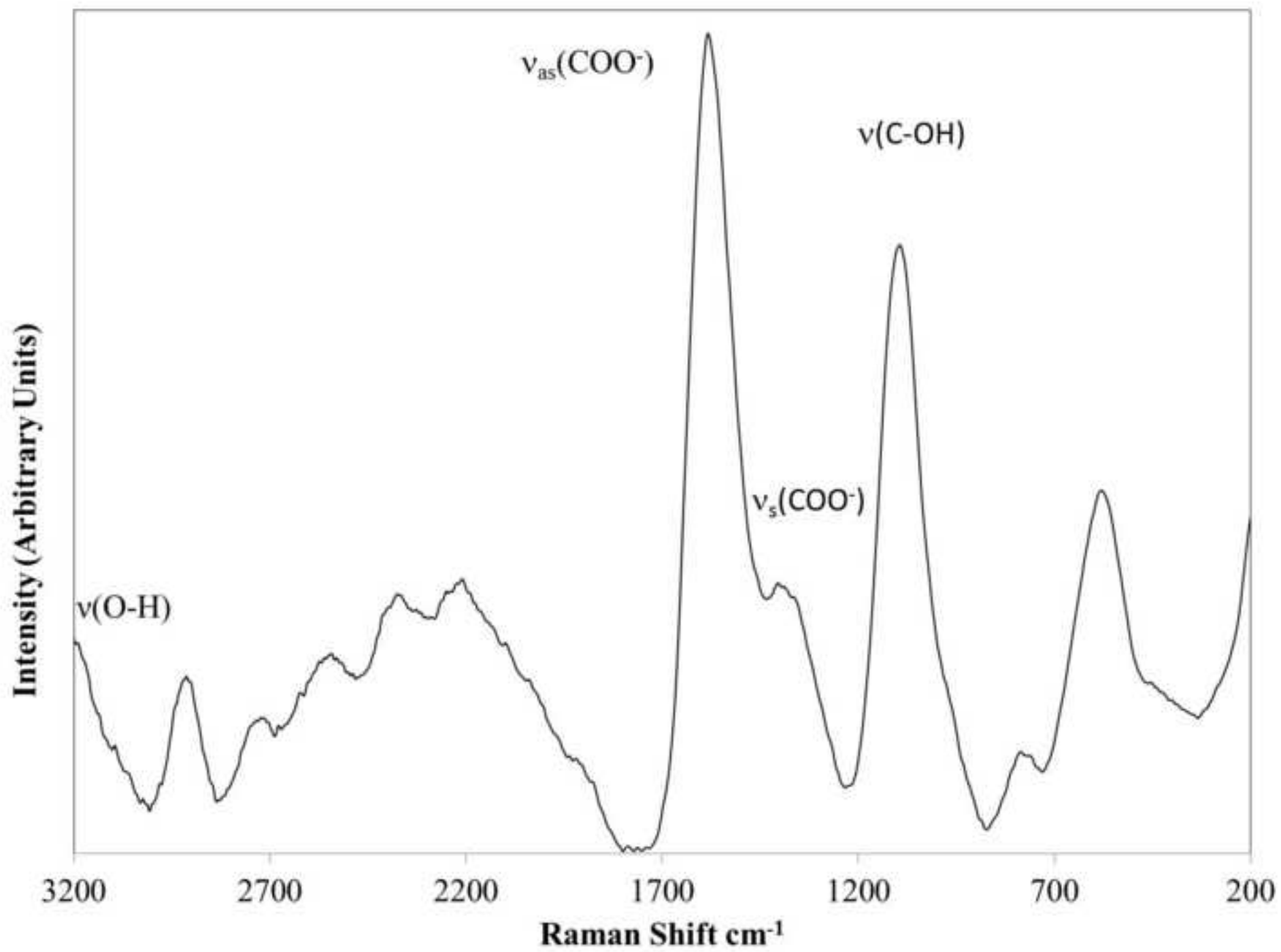
Figure(s)
[Click here to download high resolution image](#)

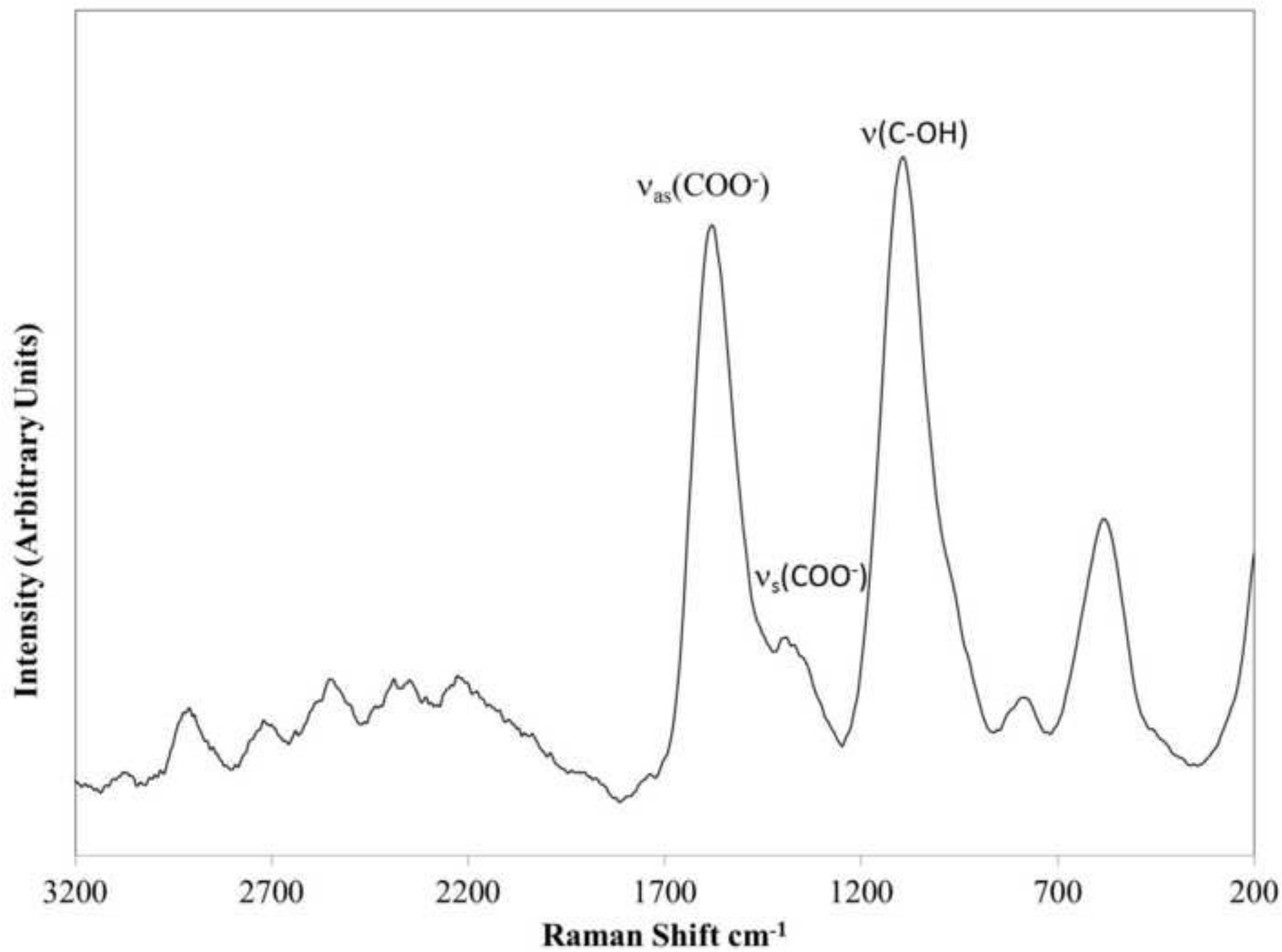


Figure(s)
[Click here to download high resolution image](#)

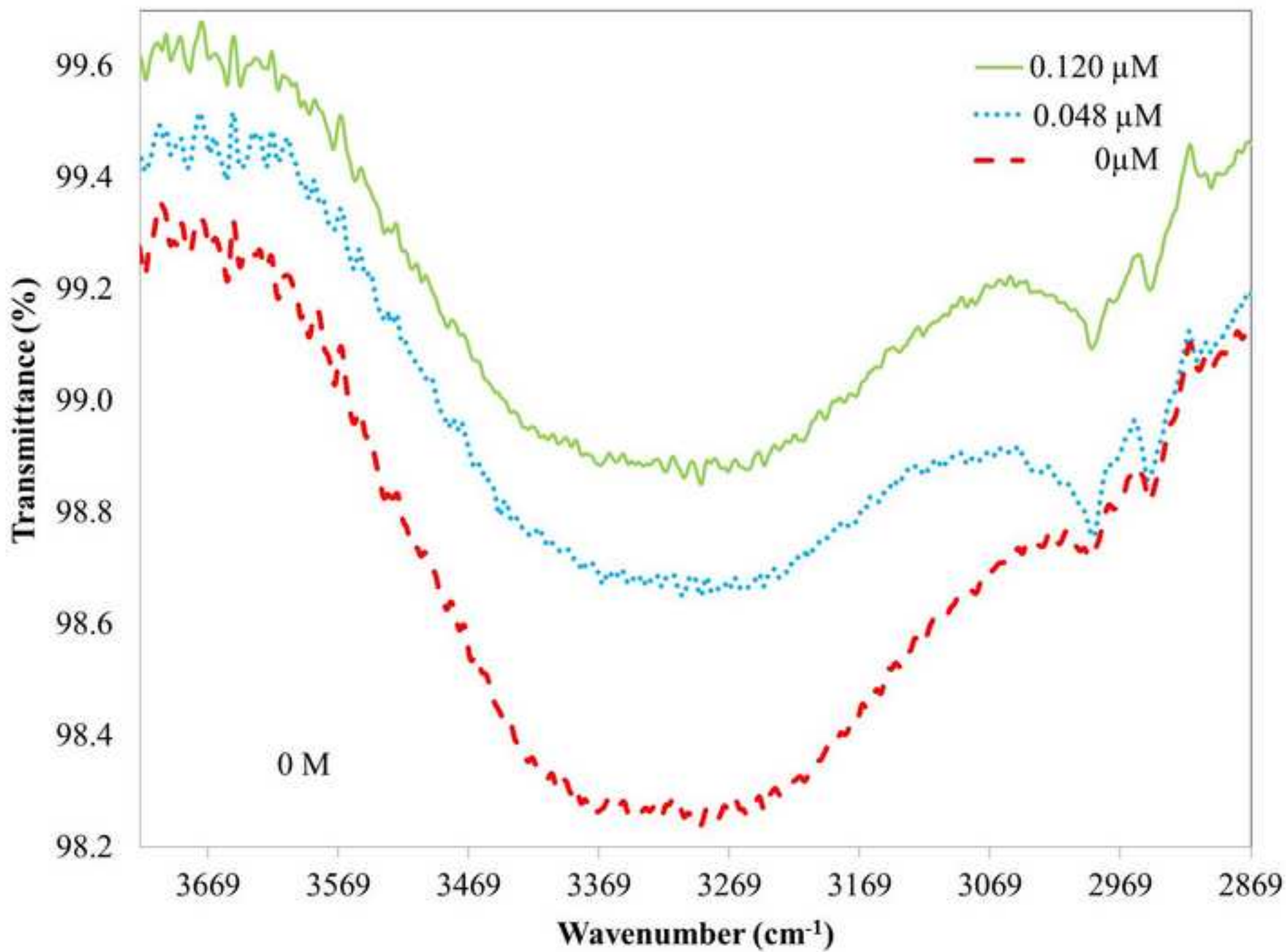


Figure(s)
[Click here to download high resolution image](#)

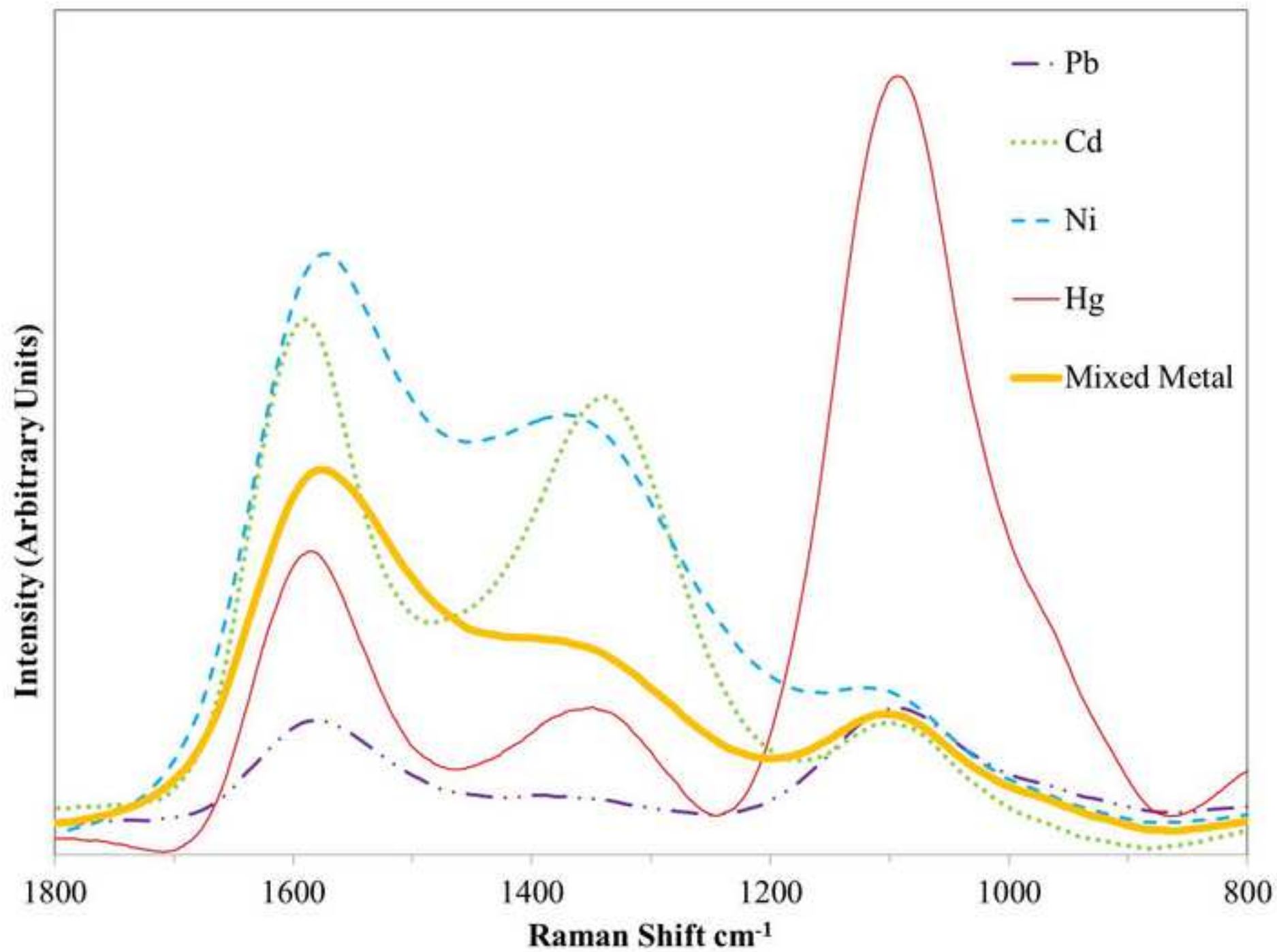




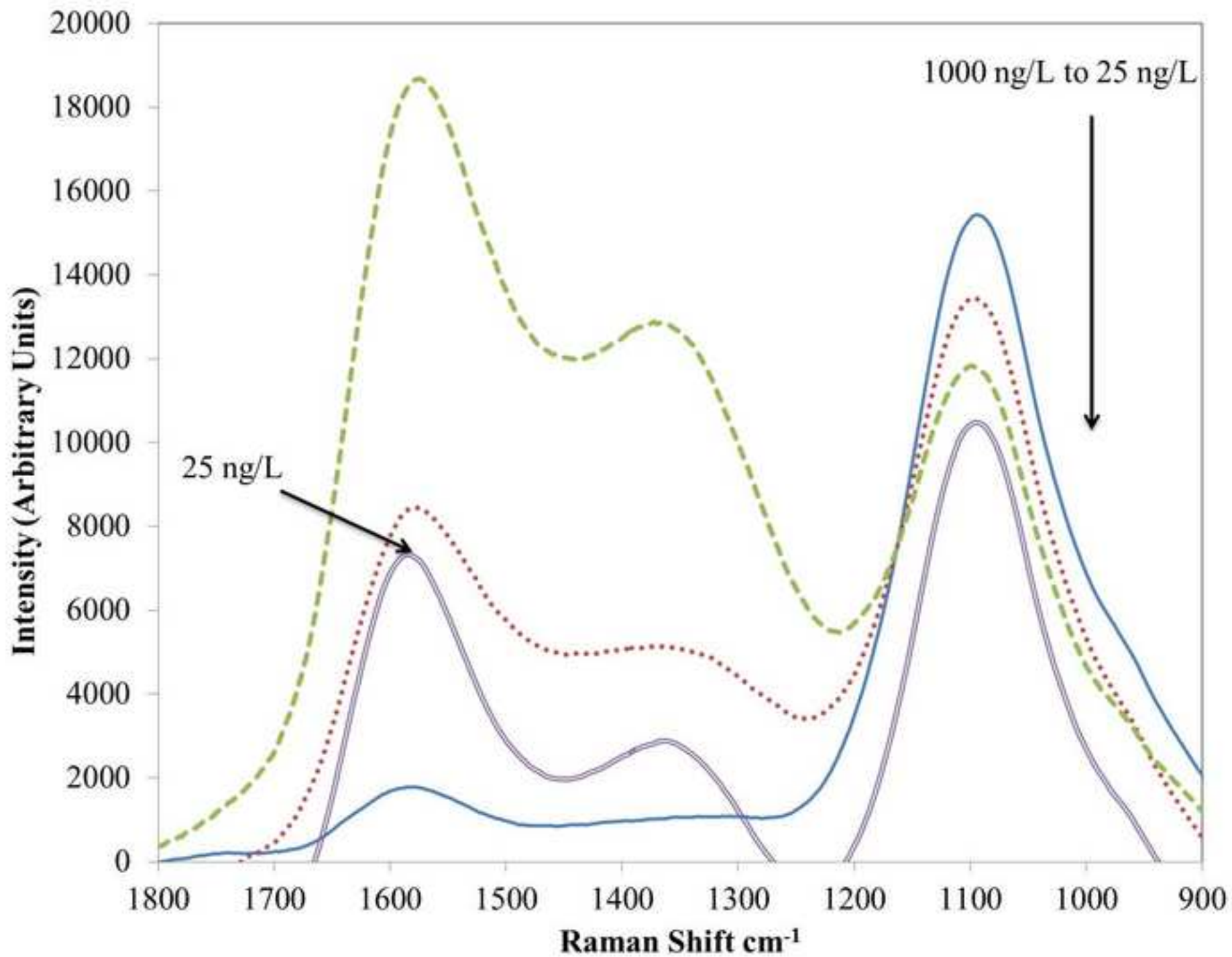
Figure(s)
[Click here to download high resolution image](#)



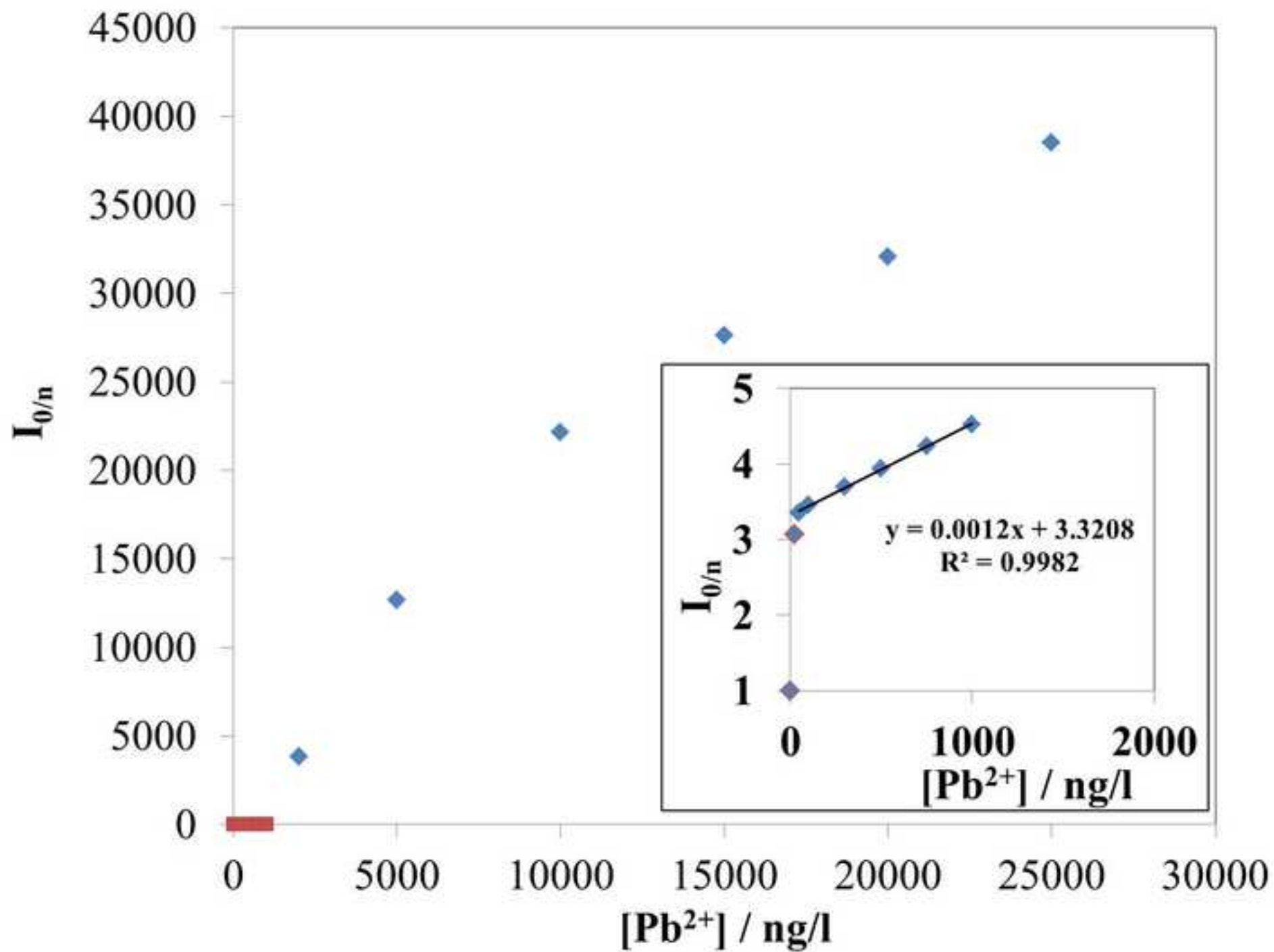
Figure(s)
[Click here to download high resolution image](#)



Figure(s)
[Click here to download high resolution image](#)



Figure(s)
[Click here to download high resolution image](#)



Figure(s)
[Click here to download high resolution image](#)

